Steel and Composite Structures, *Vol. 17, No. 4 (2014) 497-516*
DOI: http://dx.doi.org/10.12989/scs.2014.17.4.497

On the direct strength and effective yield strength method design of medium and high strength steel welded square section columns with slender plate elements

Hong-Xia Shen *

School of Civil Engineering, Xi'an University of Architecture and Technology, Xi'an 710055, PR China

(*Received August 24, 2013, Revised January 21, 2014, Accepted July 05, 2014*)

Abstract. The ultimate carrying capacity of axially loaded welded square box section members made of medium and high strength steels (nominal yield stresses varying from 345 MPa to 460 MPa), with large width-to-thickness ratios ranging from 35 to 70, is analyzed by finite element method (FEM). At the same time, the numerical results are compared with the predicted results using Direct Strength Method (DSM), modified DSM and Effective Yield Strength Method (EYSM). It shows that curve *a*, rather than curve *b* recommended in Code for design of steel structures GB50017-2003, should be used to check the local-overall interaction buckling strength of welded square section columns fabricated from medium and high strength steels when using DSM, modified DSM and EYSM. Despite all this, EYSM is conservative. Compared to EYSM and modified DSM, DSM provides a better prediction of the ultimate capacities of welded square box compression members with large width-thickness ratios over a wide range of width-thickness ratios, slenderness ratios and steel grades. However, for high strength steels (nominal yield strength greater than 460 MPa), the numerical and existent experimental results indicate that DSM over-estimates the load-carrying capacities of the columns with width-thickness ratio smaller than 45 and slenderness ratio less than 80. Further, for the purpose of making it suitable for a wider scope, DSM has been modified (called proposed modified DSM). The proposed modified DSM is in excellent agreement with the numerical and existing experimental results.

Keywords: medium and high strength steel; welded square box section; compression member; local-overall interaction buckling; ultimate carrying capacity; direct strength method; effective yield strength method, FEM

1. Introduction

Modern steel structures are developing in the direction of large-span, high-rise and super high-rise buildings in China, and this makes common carbon structural steel, such as Q235, cannot meet the needs of practical engineering, and low alloy steels Q345, Q390, Q420 and even Q460 must be used. For example, Q460E was used in Beijing National Stadium (also known as the Bird's Nest). When a column subjected to pure axial compression is fabricated from these grades of steel, for economic reasons, slender and wider welded cross-sections, which are liable to

*Corresponding author, Associate Professor, E-mail: shenhongxia88@126.com

http://www.techno-press.org/?journal=scs&subpage=8 ISSN: 1229-9367 (Print), 1598-6233 (Online)

achieve equal stabilities for both x and y axes, should be preferred, and a typical one is the welded square box section. This means that local buckling of the plate elements may occur before overall buckling and the compression members will fail in local-overall interaction buckling mode.

A large amount of research on the local and overall interaction buckling behavior of cold-formed compression members has been made (Rusch and Lindner 2001, Sputo and Tovar 2005, Tovar and Sputo 2005, Becque *et al*. 2008, Schafer 2008, de Miranda Batista 2009, Becque and Rasmussen 2009, Shahbazian and Wang 2011, 2012, Georgieva *et al*. 2012, Landesmann and Camotim 2013), and thus leading to two basic design methods for cold-formed steel members: Effective Wide Method (EWM) and Direct Strength Method (DSM). Also a few investigations have been reported on the interaction buckling experiments and numerical simulations of the welded build-up columns (Guo 1992, Usami and Fukumoto 1982, 1984, Pircher *et al*. 2002, Kwon *et al*. 2007, Chen 2009, Degée *et al*. 2008, Shen 2012). Meanwhile, these studies have developed EWM, DSM and EYSM, and made them suitable for welded box-, H- and channel- cross-sections. However, most of the previous studies are not in-depth and comprehensive enough to cover a wide range of steel types and grades, on the other hand, simpler and newly developed design methods, such as DSM and EYSM, for welded thin-walled sections still need to be improved, therefore, further studies are necessary. Shen (2012) developed a double nonlinear (i.e., geometric and material nonlinear) finite element model taking the geometric imperfections and residual stresses into consideration by using ANSYS program and the ultimate carrying capacity of axially loaded welded box section members made of Q235 steel, with slender plate elements, is modeled, and the DSM was proved to be accurate in predicting the ultimate strength of welded box section columns. In this paper, this finite element model is extended for medium and high strength steel (nominal yield stress varying from 345 MPa to 460 MPa) columns, and the numerical results are compared with two simpler design methods, namely DSM and EYSM, so as to evaluate the applicability of the two techniques.

2. Geometric model

2.1 Research object

Research object of this paper focuses on a pin-ended steel member subjected to axial load, with square box section fabricated from plate elements welded together at the corners. The geometric dimensions of the cross-section are shown in Fig. 1(a). Although the plate thickness is possible to affect the behavior of the compression members, a welded thin-walled section is studied in this paper and its influence is small. Therefore, for all the simulation objects, the thickness of plate elements, t = 4 mm. The ranges of the other parameters are summarized as follows:

(1) Steel grade: Q345, Q390, Q420 and SM58. SM58 is Japanese steel, the nominal yield stress of which is 460 MPa, and equivalent to Chinese Q460 steel, So Q460 is not included in this study.
(2) Two types of cross-sections: non-slender element sections and slender-element sections. The non-slender sections are simulated to determine the type of the column curve, that is to say, which one the welded square section should be when checking the global stability without local plate buckling. The slender sections are used to investigate the local-overall interaction buckling behavior.
(3) Slender ratio, $\lambda = l/i$ = 20, 40, 60 and 80 (l is the column length, i is the radius of gyration of

the cross-section about the buckling axis).

(4) Plate width-to-thickness ratio, b/t = 29, 30, 31 and 33 for non-slender sections; b/t = 35, 40, 45, 50, 55, 60 and 70 for slender sections.

2.2 Initial imperfection

Two kinds of initial imperfections, namely residual stresses and initial curvatures, are taken into account. Residual stress measurements of the welded square box section were made by Usami and Fukumoto (1984). SM58 steel plate of 4.5 mm thickness was used, the nominal yield strength of which is 460 MPa and the measured yield strength is 568 MPa. The width-to-thickness ratio, b/t = 29, 44 and 58. Measured residual stress patterns were all similar in shape to the well-known pattern, tensile stresses about 80% of the measured yield strength (i.e., $0.8 \times 568 = 454$ MPa, which is very close to the nominal yield strength of 460 MPa) were measured near the corners and nearly constant compressive stresses were observed over the central portion of each plate. The average values of the measured compressive stresses were 32%, 22% and 15% of the measured yield strength for specimens with b/t = 29, 44 and 58, respectively. As a result, the uniform residual stress distribution model is adopted for all the steel grades in this study. Because of the similar residual stress distributions on four plates of the cross-section, only one of them is plotted in simplified pattern (Chen 1992) in Fig. 1(b), where tensile residual stresses are designated as positive and compressive stresses as negative. Tensile residual stresses near the weld, with a magnitude equal to the nominal yield strength, f_y, extend over a width of $c = 3t$. According to the equilibrium condition, the magnitude of compressive residual stresses is equal to

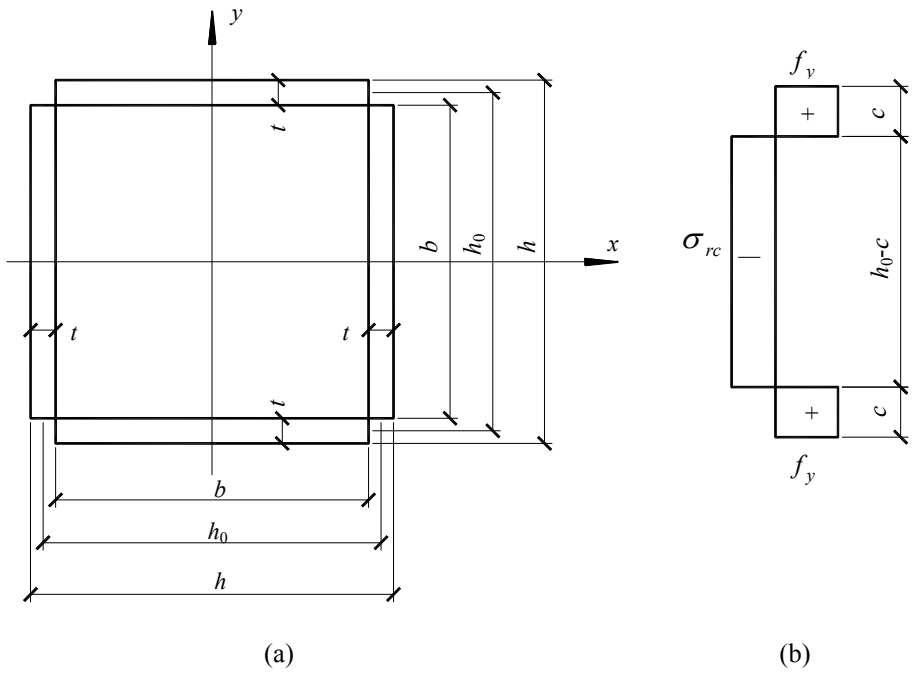

Fig. 1 Welded box-shaped section: (a) Geometric dimension; (b) Residual stress distribution

$$\sigma_{rc} = \frac{2c}{h_0 - 2c} f_y \tag{1}$$

where h_0 is the distance between the centre lines of the two opposite plates (see Fig. 1(a)).

Both the global and local initial deflections are taken into account. The global initial curvature is taken as a half-wave sine curve with amplitude of $l/1000$. Due to the similarity of the four plate elements, no interaction exists between the two adjacent plates and any of them may be regarded as simply supported at its four edges. Thus, making use of a coordinate system shown in Fig. 1(a), the forms of local initial deflections are assumed as follows

$$\omega = \omega_0 \sin\frac{m\pi z}{l}\cos\frac{\pi x}{b} \qquad (y = \pm h_0/2) \tag{2a}$$

or

$$\omega = \omega_0 \sin\frac{m\pi z}{l}\cos\frac{\pi y}{b} \qquad (x = \pm h_0/2) \tag{2b}$$

where b is the plate width; $m = l/b$, which is the buckling half-wave number along the axial direction (z-direction) of a member; and ω_0, the magnitude of initial imperfection in local mode, which is taken as $b/1000$ (Degée *et al*. 2008).

3. Finite element model and verification

3.1 Finite element model

Finite element model was developed using the commercial program ANSYS 8.0 (Swanson Analysis Systems Inc 2004). Two elements were used: Beam189 as well as Shell181 for the non-slender sections to verify the simulation results using Shell181, and only Shell181 for the slender sections to consider the influence of local buckling. The stress-strain relationships measured for SM58 steel were similar to those for mild steel (Usami and Fukumoto 1984), hence all the steel materials were assumed to be elastic-perfectly plastic. The nominal yield strength, Young's modulus $E = 206{,}000$ MPa and Poisson's ratio $v = 0.3$ were used for Q345, Q390 and Q420 steels, while the measured material properties for SM58.

The modeling of the compression members with slender-plate sections is of importance. For the purpose of taking account of geometric imperfections, i.e., global and local initial deflections, direct modelling method was used. The number of nodes required and the order in which they should be generated were determined firstly, and then all nodes were generated according to the x, y, and z coordinates considering geometric imperfections. Further, the element attributes (element type, material, and real constant) having been set, shell elements were automatically generated within each area defined by four nodes. For any plate in a box section column, element size was $h_0/8$ along its width and $h_0/4$ in longitudinal direction, and thus the grid was $h_0/8 \times h_0/4$. In this study, the minimum grid was approximately 14.5 mm × 29 mm and the maximum one 35 mm × 70 mm, which satisfied the accuracy requirement. Fig. 2 shows the initial geometric imperfections imposed by direct modelling, in which the initial deflections are enlarged 5000 times in order to observe clearly. Residual stress was treated as initial stress, which is a loading and must be specified at all integration points of shell or beam elements in ANSYS software (Swanson

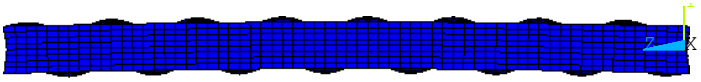

Fig. 2 Initial geometric imperfections imposed by direct modelling

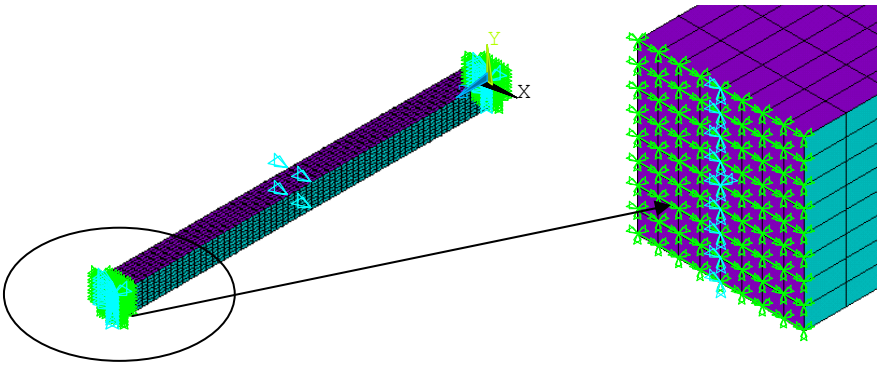

Fig. 3 Typical finite element model: (a) Shell element model; (b) End boundary conditions

Analysis Systems Inc. 2004). An end plate with a thickness of 30 mm was attached to both ends of a member, on which the boundary conditions were applied, to ensure that the two ends of the columns were hinged. Fig. 3 is a typical finite element model and the detailed modeling process may be found in the literature (Shen 2012).

3.2 Verification of the finite element model

In order to verify the finite element model mentioned above, a total of thirty-two experimental specimens, of which twenty-one were centrally loaded, eleven were eccentrally loaded (Usami and Fukumoto 1982, 1984) are simulated firstly. Material properties, residual stresses, and initial deflections as measured by Usami and Fukumoto (1982, 1984) are adopted. The numerical results are listed in Table 1. "E" refers to the specimens loaded with equal eccentricity, $e_1 = i/4$ or $e_2 = i/2$; "S" the specimens having square box sections, and "R" the specimens having rectangular box sections. The number following S, R, ES and ER is the value of slenderness ratio, and the last number is the value of width-to-thickness ratio of the flange plates. In Table 1, φ_1 and φ_2 represent the stability reduction factors obtained from the experiment and FEM analysis, respectively. Comparison shows that the numerical results agree very well with the experimental results, indicating that the finite element model provided in this study can accurately predict the local and overall interaction buckling strength of welded box columns.

4. Analysis of the numerical results

4.1 Non-slender sections

In this section, non-slender sections are simulated additionally for two reasons, one for verifying

Table 1 Comparison between the numerical and experimental results (Usami and Fukumoto 1982, 1984)

No.	Specimen	φ_1	φ_2	φ_2/φ_1	No.	Specimen	φ_1	φ_2	φ_2/φ_1
1	S-35-22	0.852	0.829	0.973	17	R-40-44	0.644	0.651	1.011
2	S-35-33	0.722	0.732	1.014	18	R-40-58	0.498	0.484	0.972
3	S-35-38	0.621	0.626	1.008	19	R-65-29	0.619	0.654	1.057
4	S-35-44	0.544	0.549	1.009	20	R-65-44	0.521	0.533	1.023
5	S-50-22	0.740	0.694	0.938	21	R-65-58	0.441	0.462	1.048
6	S-50-27	0.672	0.684	1.018	22	ER-40-29e_1	0.610	0.618	1.012
7	S-50-33	0.670	0.708	1.057	23	ER-40-44e_1	0.501	0.500	0.997
8	R-50-22	0.743	0.687	0.925	24	ER-40-58e_1	0.391	0.413	1.056
9	R-50-27	0.731	0.678	0.928	25	ER-40-44e_2	0.411	0.422	1.027
10	R-50-33	0.709	0.699	0.986	26	ER-65-29e_1	0.435	0.438	1.006
11	R-50-38	0.639	0.687	1.075	27	ER-65-44e_1	0.406	0.426	1.049
12	R-50-44	0.579	0.589	1.017	28	ER-65-58e_1	0.312	0.334	1.071
13	R-65-22	0.593	0.594	1.002	29	ER-65-44e_2	0.325	0.351	1.079
14	R-65-27	0.637	0.574	0.901	30	ER-65-58e_2	0.268	0.284	1.059
15	R-65-33	0.585	0.613	1.048	31	ES-40-44e_1	0.441	0.478	1.084
16	R-40-29	0.798	0.770	0.965	32	ES-40-58e_1	0.363	0.359	0.988

the numerical results of Shell181 element further, and the other for checking whether the column strength curves based on mild steel, given in Code for design of steel structures GB50017-2003, are suitable for medium and high strength steels or not. According to the Chinese Code GB50017-2003, the width-to-thickness ratio of the plate elements preferably should not be greater than $40\sqrt{235/f_y}$ (f_y is nominal yield strength of steel) when a box-shaped member is subjected to a centric axial load. Therefore, the width-to-thickness ratio limit values of the component plate elements are 33, 31, 30 and 29 for Q345, Q390, Q420 and SM58 steels, respectively.

4.1.1 Comparison between the numerical results with elements Beam189 and Shell181

Due to few of medium-long columns in the tests (Usami and Fukumoto 1982, 1984), for b/t = 29 sections, Beam189 element, together with Shell181, is selected to check the numerical results of the medium-long members using Shell181. Fig. 4 describes the curves of load carrying capacity versus axial compressive deformation, U_z, with two different elements Beam189 and Shell181. As can be noticed in Fig. 4, the ultimate bearing capacities obtained from Shell181 are very close to those from Beam189. The maximum carrying capacities are also given in Table 2, which are expressed as the stability reduction coefficients, φ_3, numerical results by Shell181 and φ_4, by Beam189. The values of φ_3/φ_4 change from 0.995 to 1.052. The ultimate strengths by two different methods are in good agreement. In addition, the load-deformation curves using Shell181 are in good accordance with those using Beam189 before the ultimate capacities. However, after reaching the maximum carrying capacities, the curves from Shell181 descend more slowly than the ones from Beam189 except for λ = 20. This may because that Shell181 has membrane stiffness besides bending stiffness compared to Beam189, and the membrane tension plays an important role in delaying the deterioration of flexural rigidity of Shell181.

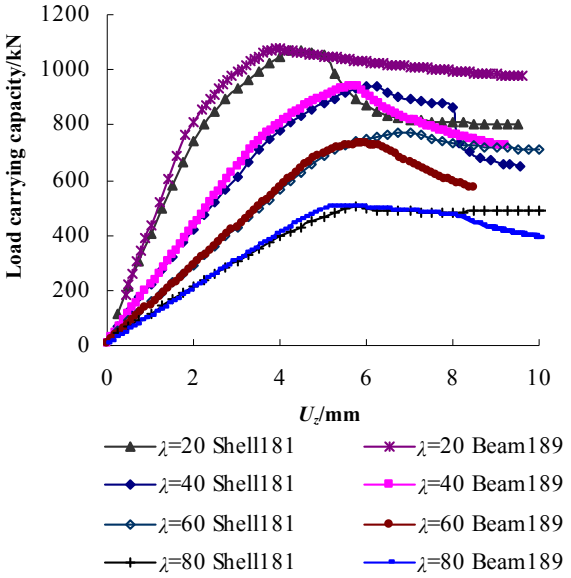

Fig. 4 Comparison of numerical results using elements Shell181 and Beam189

Table 2 Comparison of numerical results by elements Shell181 and Beam189 (SM58 steel)

λ	φ_3	φ_4	φ_3/φ_4
20	0.982	0.987	0.995
40	0.865	0.860	1.005
60	0.705	0.670	1.052
80	0.462	0.462	1.000

4.1.2 Comparison between the numerical results and Chinese standard

Table 3 gives the numerical simulation results, φ_5, by Shell181 element when the columns loaded to fail in the overall flexural buckling mode, in which residual stresses and initial curvature are all taken into account. Also shown in Table 3 are the stability reduction coefficients, φ_a and φ_b, obtained from column design curve *a* and *b*, respectively, according to Chinese code GB50017-2003. It can be found from Table 3 that the values of φ_5/φ_a range from 0.98 to 1.13 with an average value of 1.05 and those of φ_5/φ_b change from 1.05 to 1.29 with a mean value of 1.14. All results are higher than the design curve *b* recommended by the Chinese current standard and most of them even more than the curve *a*. Since the average value, not the minimum value, is used to determine the column strength curves in code GB50017-2003, curve *b* should be replaced by curve *a* to predict the column overall strength without local plate buckling when the width-thickness ratio of box sections is greater than 20. The similar conclusion, which is the use of curve *a* instead of curve *b* recommended by EN 1993-1-1, was drawn by Degée *et al*. (2008), when the local and global interaction buckling of welded box section compression members made of S355, S460 and S690 steels was investigated. Although there is a little difference in the value of the equivalent imperfection between GB50017-2003 and EN 1993-1-1 when determining the stability reduction factor, the values of three design column curves *a*, *b*, *c* in GB50017-2003 approach to three design

Table 3 Comparison of numerical results using element Shell181 and Chinese standard

Steel grade and width-thickness ratio limit value	λ	φ_5	φ_a	φ_b	φ_5/φ_a	φ_5/φ_b
Q345 (b/t = 33)	20	1.081	0.974	0.957	1.11	1.13
	40	0.989	0.923	0.868	1.07	1.14
	60	0.847	0.834	0.745	1.02	1.14
	80	0.698	0.653	0.568	1.07	1.23
Q390 (b/t = 31)	20	1.031	0.972	0.953	1.06	1.08
	40	0.936	0.916	0.856	1.02	1.09
	60	0.814	0.810	0.717	1.00	1.14
	80	0.665	0.607	0.529	1.10	1.26
Q420 (b/t = 30)	20	1.078	0.970	0.950	1.11	1.13
	40	0.955	0.910	0.847	1.05	1.13
	60	0.776	0.787	0.697	0.99	1.11
	80	0.650	0.577	0.505	1.13	1.29
SM58 (b/t = 29)	20	0.982	0.962	0.934	1.02	1.05
	40	0.865	0.879	0.802	0.98	1.08
	60	0.705	0.703	0.614	1.00	1.15
	80	0.462	0.459	0.406	1.01	1.14
Average value					1.05	1.14

column curves of *a*, *b* and *c* of EN 1993-1-1. As a result, a suggestion is made that, in the case of $b/t > 20$, curve *a*, rather than curve *b*, in GB50017-2003 should be used to check the global stability of welded square section columns fabricated from Q345, Q390, Q420, and SM58 steels.

4.2 Slender sections

For Q345, Q390 and Q420 steel grades, the width-thickness ratios, b/t, are taken as 40, 50, 60 and 70, and for SM58 steel, b/t ratios are 35, 40, 45, 50, 55 and 60, which are all greater than the width-thickness ratio limit corresponding to each steel grade. In the meantime, for a long column, the overall flexural deformation plays a leading role in the interaction buckling (Shen 2012), and the effects of the local buckling on the column maximum strength were large in the regions of small slenderness ratio, but almost diminished in the regions of large slenderness (Usami and Fukumoto 1982). Numerical ranges of the slenderness, λ, were not provided by Usami and Fukumoto, but from Figs. 9 and 10 in his paper it could be found that when the λ was greater than 70 the influence of the b/t was very small. Thereby, the slenderness ratios, λ, are limited to the range of 20 to 80, i.e., λ = 20, 40, 60 and 80, in this paper. The ultimate load carrying capacities, P_u, of these compression members are computed using the developed finite element model and listed in Tables 4-7.

4.2.1 DSM and modified DSM

DSM, proposed by Schafer (Rusch and Lindner 2001), has been used for the design of

cold-formed steel sections formally (AISI 2004). In recent years, along with the rapid development of DSM, it was modified (called modified DSM) by Kwon *et al*. (2007), and applied to the welded thin-walled sections. Furthermore, modified DSM has been proved to be capable of predicting accurately the ultimate strength of welded H and channel section columns with nominal yield strength of 240 MPa. Also DSM and modified DSM are suitable for welded square box columns made of mild steel (nominal yield strength is 235 MPa), and modified DSM is a more reasonable predictor of strength than DSM over a wide range of width-to-thickness ratios (Shen 2012). So, in this study, two approaches are used for medium and high strength steels.

The load-carrying capacity of a compression member can be calculated using DSM through the following formulas (AISI 2004)

$$\text{when} \quad \lambda_l \le 0.776 \qquad P_l = P_m \tag{3a}$$

$$\text{when} \quad \lambda_l > 0.776 \qquad P_l = \left[1 - 0.15\left(\frac{P_{cr,l}}{P_m}\right)^{0.4}\right]\left(\frac{P_{cr,l}}{P_m}\right)^{0.4} P_m \tag{3b}$$

$$\lambda_l = \sqrt{P_m / P_{cr,l}} \tag{4}$$

where P_l is the load-carrying capacity of a column calculated using DSM;

P_m is the overall stability capacity and expressed as

$$P_m = \varphi A f_y \tag{5}$$

$P_{cr,l}$ is the local buckling load and given by

$$P_{cr,l} = \sigma_{cr,l} A \tag{6}$$

in which φ is the overall stability reduction factor, A is cross-section area, and $\sigma_{cr,l}$ is the critical stress of a plate under uniform compression, and for a plate simply supported on four edges, it can be expressed as

$$\sigma_{cr,l} = \frac{4\pi^2 E}{12(1-\nu^2)}\left(\frac{t}{b}\right)^2 \tag{7}$$

Eqs. (3a)-(3b) were modified by Kwon *et al*. (2007) and expressed as follows

$$\text{when} \quad \lambda_l \le 0.816 \qquad P_l = P_m \tag{8a}$$

$$\text{when} \quad \lambda_l > 0.816 \qquad P_l = \left[1 - 0.15\left(\frac{P_{cr,l}}{P_m}\right)^{0.5}\right]\left(\frac{P_{cr,l}}{P_m}\right)^{0.5} P_m \tag{8b}$$

The predicted values, P_{l1}, from Eqs. (3)-(7), and P_{l2}, from Eqs.(8a)-(8b) are compared with the numerical results, P_u, as shown in Tables 4-7. In all the tables, ε_1 and ε_2 are the errors expressed as a percentage, i.e., $\varepsilon_1 = \frac{P_u - P_{l1}}{P_{l1}} \times 100\%$, and $\varepsilon_2 = \frac{P_u - P_{l2}}{P_{l2}} \times 100\%$. It can be seen, from these tables,

Table 4 Comparisons between FEM and DSM, FEM and modified DSM, FEM and EYSM (Q345 steel)

λ	b/t =40									b/t =50								
	P_u/kN	P_{l1}/kN	P_{l2}/kN	N_1/kN	N_2/kN	ε_1/%	ε_2/%	ε_3/%	ε_4/%	P_u/kN	P_{l1}/kN	P_{l2}/kN	N_1/kN	N_2/kN	ε_1/%	ε_2/%	ε_3/%	ε_4/%
20	857.27	832.84	854.55	799.84	805.75	2.93	0.32	7.18	6.39	876.18	895.80	886.84	843.61	848.01	-2.19	-1.20	3.86	3.32
40	857.76	802.78	827.01	759.68	778.21	6.85	3.72	12.91	10.22	849.85	864.21	859.44	807.42	820.61	-1.66	-1.12	5.26	3.56
60	763.69	748.78	755.00	691.67	728.27	1.99	1.15	10.41	4.86	802.65	807.44	809.75	747.10	770.91	-0.59	-0.88	7.44	4.12
80	636.69	591.15	591.15	572.84	591.15	7.70	7.70	11.15	7.70	734.27	684.34	699.72	646.28	660.87	7.29	4.94	13.62	11.11
λ	b/t =60									b/t =70								
	P_u /kN	P_{l1}/kN	P_{l2}/kN	N_1/kN	N_2/kN	ε_1/%	ε_2/%	ε_3/%	ε_4/%	P_u /kN	P_{l1}/kN	P_{l2}/kN	N_1/kN	N_2/kN	ε_1/%	ε_2/%	ε_3/%	ε_4/%
20	967.00	946.99	908.17	872.68	875.94	2.11	6.48	10.81	10.40	1011.59	990.29	923.31	895.74	895.76	2.15	9.56	12.93	12.93
40	941.22	914.11	880.86	839.77	848.62	2.97	6.85	12.08	10.91	1004.22	956.29	896.07	862.09	868.51	5.01	12.07	16.49	15.63
60	862.89	855.01	831.33	788.17	799.08	0.92	3.80	9.48	7.98	924.35	895.17	846.65	818.44	819.09	3.26	9.18	12.94	12.85
80	743.63	726.79	721.66	701.88	689.40	2.32	3.04	5.95	7.87	804.17	762.50	737.24	743.87	709.66	5.46	9.08	8.11	13.32

Note: The averages of ε_1, ε_2, ε_3 and ε_4 are 2.91%, 4.67%, 10.04% and 8.95%, respectively, and the standard deviations of ε_1, ε_2, ε_3 and ε_4 are 2.99%, 4.24%, 3.49% and 3.81%, respectively

Table 5 Comparisons between FEM and DSM, FEM and modified DSM, FEM and EYSM (Q390 steel)

λ	b/t =40									b/t =50								
	P_u/kN	P_{l1}/kN	P_{l2}/kN	N_1/kN	N_2/kN	ε_1/%	ε_2/%	ε_3/%	ε_4/%	P_u/kN	P_{l1}/kN	P_{l2}/kN	N_1/kN	N_2/kN	ε_1/%	ε_2/%	ε_3/%	ε_4/%
20	865.40	903.99	919.02	862.95	870.23	-4.27	-5.83	0.28	-0.55	946.54	970.55	951.00	906.52	912.18	-2.47	-0.47	4.41	3.77
40	859.40	868.30	886.80	815.99	838.00	-1.02	-3.09	5.32	2.55	915.04	933.06	918.94	864.77	880.11	-1.93	-0.42	5.81	3.97
60	804.08	798.40	822.99	734.49	774.18	0.71	-2.30	9.48	3.86	836.14	859.60	855.43	796.11	816.60	-2.73	-2.26	5.03	2.39
80	681.26	621.18	621.18	591.84	621.18	9.67	9.67	15.11	9.67	758.48	707.79	720.93	675.48	682.08	7.16	5.21	12.29	11.20

Table 5 Continued

λ	b/t =60									b/t =70								
	P_u /kN	P_{l1}/kN	P_{l2}/kN	N_1/kN	N_2/kN	ε_1/%	ε_2/%	ε_3/%	ε_4/%	P_u /kN	P_{l1}/kN	P_{l2}/kN	N_1/kN	N_2/kN	ε_1/%	ε_2/%	ε_3/%	ε_4/%
20	1032.19	1024.78	972.12	937.37	939.89	0.72	6.18	10.12	9.82	1106.93	1070.72	987.11	958.58	959.56	3.38	12.14	15.48	15.36
40	999.52	985.77	940.16	897.24	907.93	1.40	6.31	11.40	10.09	1085.43	1030.38	955.23	922.50	927.67	5.34	13.63	17.66	17.01
60	919.34	909.32	876.87	839.91	844.63	1.10	4.84	9.46	8.85	988.25	951.33	892.08	871.79	864.52	3.88	10.78	13.36	14.31
80	792.23	751.22	742.80	735.76	710.55	5.46	6.65	7.68	11.49	848.76	787.78	758.33	786.96	730.76	7.74	11.93	7.85	16.15

Note: The averages of ε_1, ε_2, ε_3 and ε_4 are 2.13%, 4.56%, 9.42% and 8.75%, respectively, and the standard deviations of ε_1, ε_2, ε_3 and ε_4 are 4.14%, 6.22%, 4.68% and 5.49%, respectively

Table 6 Comparisons between FEM and DSM, FEM and modified DSM, FEM and EYSM (Q420 steel)

λ	b/t =40									b/t =50								
	P_u/kN	P_{l1}/kN	P_{l2}/kN	N_1/kN	N_2/kN	ε_1/%	ε_2/%	ε_3/%	ε_4/%	P_u/kN	P_{l1}/kN	P_{l2}/kN	N_1/kN	N_2/kN	ε_1/%	ε_2/%	ε_3/%	ε_4/%
20	915.80	949.15	959.45	902.21	910.66	-3.51	-4.55	1.51	0.56	1017.96	1017.97	991.23	947.56	952.41	-0.00	2.70	7.43	6.88
40	883.90	909.03	923.55	853.01	874.75	-2.76	-4.29	3.62	1.05	965.83	975.84	955.51	901.00	916.68	-1.03	1.08	7.19	5.36
60	830.58	823.52	846.04	759.27	797.23	0.86	-1.83	9.39	4.18	864.65	886.01	878.37	828.26	839.54	-2.41	-1.56	4.39	2.99
80	712.80	664.82	635.90	606.11	649.27	7.22	12.09	17.60	9.79	768.36	719.12	731.14	692.48	692.29	6.85	5.09	10.96	10.99
λ	b/t =60									b/t =70								
	P_u /kN	P_{l1}/kN	P_{l2}/kN	N_1/kN	N_2/kN	ε_1/%	ε_2/%	ε_3/%	ε_4/%	P_u /kN	P_{l1}/kN	P_{l2}/kN	N_1/kN	N_2/kN	ε_1/%	ε_2/%	ε_3/%	ε_4/%
20	1141.50	1074.11	1012.22	976.45	979.99	6.27	12.77	16.90	16.48	1236.77	1121.71	1027.12	997.61	999.57	10.26	20.41	23.97	23.73
40	1082.35	1030.28	976.61	934.55	944.38	5.05	10.83	15.81	14.61	1191.34	1076.40	991.59	959.98	964.04	10.68	20.14	24.10	23.58
60	966.75	936.81	899.73	868.73	867.49	3.20	7.45	11.28	11.44	1055.72	979.76	914.89	901.00	887.33	7.75	15.39	17.17	18.98
80	827.86	763.03	752.98	761.01	720.73	8.50	9.94	8.78	14.86	908.52	800.00	768.48	802.36	740.91	13.56	18.22	13.23	22.62

Note: The averages of ε_1, ε_2, ε_3 and ε_4 are 4.41%, 7.74%, 12.08% and 11.76%, respectively, and the standard deviations of ε_1, ε_2, ε_3 and ε_4 are 5.33%, 8.53%, 6.78% and 7.90%, respectively

Table 7 Comparisons between FEM and DSM, FEM and modified DSM, FEM and EYSM (SM58 steel)

λ	b/t =35									b/t =40								
	P_u/kN	P_{l1}/kN	P_{l2}/kN	N_1/kN	N_2/kN	ε_1/%	ε_2/%	ε_3/%	ε_4/%	P_u/kN	P_{l1}/kN	P_{l2}/kN	N_1/kN	N_2/kN	ε_1/%	ε_2/%	ε_3/%	ε_4/%
20	987.03	1104.95	1113.78	1049.78	1061.88	-10.67	-11.38	-5.98	-7.05	1038.27	1152.09	1135.85	1081.48	1091.35	-9.88	-8.59	-4.00	-4.86
40	953.80	1039.61	1055.46	973.63	1003.29	-8.25	-9.63	-2.04	-4.93	973.27	1084.84	1077.73	1011.10	1033.69	-10.28	-9.69	-3.74	-5.84
60	877.78	892.78	920.00	815.89	869.11	-1.68	-4.59	7.59	1.00	884.37	933.65	944.63	868.09	878.13	-5.28	-6.38	1.88	0.71
80	674.03	598.06	600.68	585.26	600.68	12.70	12.21	15.17	12.21	745.58	684.11	684.11	646.88	683.06	8.99	8.99	15.26	9.15
λ	b/t =45									b/t =50								
	P_u /kN	P_{l1}/kN	P_{l2}/kN	N_1/kN	N_2/kN	ε_1/%	ε_2/%	ε_3/%	ε_4/%	P_u /kN	P_{l1}/kN	P_{l2}/kN	N_1/kN	N_2/kN	ε_1/%	ε_2/%	ε_3/%	ε_4/%
20	1128.32	1193.60	1152.89	1106.87	1114.11	-5.47	-2.13	1.94	1.28	1203.30	1230.75	1166.45	1126.71	1132.22	-2.23	3.16	6.80	6.28
40	1046.14	1124.62	1094.93	1039.61	1055.89	-6.98	-4.46	0.63	-0.92	1121.03	1160.20	1108.61	1064.18	1074.12	-3.38	1.12	5.34	4.37
60	905.40	969.51	962.19	913.08	922.53	-6.61	-5.90	-0.84	-1.86	931.11	1001.51	976.16	949.54	920.86	-7.03	-4.61	-1.94	1.11
80	760.04	727.10	746.58	703.33	705.94	4.53	1.80	8.06	7.66	799.06	753.37	761.02	753.84	724.93	6.06	5.00	6.00	10.23
λ	b/t =55									b/t =60								
	P_u /kN	P_{l1}/kN	P_{l2}/kN	N_1/kN	N_2/kN	ε_1/%	ε_2/%	ε_3/%	ε_4/%	P_u /kN	P_{l1}/kN	P_{l2}/kN	N_1/kN	N_2/kN	ε_1/%	ε_2/%	ε_3/%	ε_4/%
20	1284.52	1264.41	1177.48	1143.36	1146.97	1.59	9.09	12.35	11.99	1357.46	1295.22	1186.65	1156.45	1159.21	4.81	14.39	17.38	17.10
40	1186.81	1192.41	1119.76	1082.38	1088.98	-0.47	5.99	9.65	8.98	1264.03	1221.88	1129.01	1099.58	1101.31	3.45	11.96	14.96	14.78
60	1010.73	1030.43	987.53	979.19	956.95	-1.91	2.35	3.22	5.62	1071.61	1056.85	996.98	1004.79	968.68	1.40	7.49	6.65	10.63
80	842.06	777.03	772.78	798.60	740.41	8.37	8.97	5.44	13.73	891.88	798.58	782.54	837.72	753.26	11.68	13.97	6.47	18.40

Note: The averages of ε_1, ε_2, ε_3 and ε_4 are -0.67%, 1.63%, 5.26% and 5.41%, respectively, and the standard deviations of ε_1, ε_2, ε_3 and ε_4 are 7.07%, 8.19%, 6.63% and 7.52%, respectively

that DSM is more accurate than modified DSM in predicting the ultimate strength of compression members with slender plates over a wide range of steel types, slenderness and width-to-thickness ratios. In the case of medium-high strength steels, such as Q345 and Q390, DSM and modified DSM can be able to estimate the local-overall buckling strength of centrically loaded members precisely. But for Q420, modified DSM underestimates the column strength for large width-to-thickness ratio (i.e., b/t = 60 and 70) members, while DSM agrees well. In the case of high strength steel, like SM58, an overestimation is made when DSM and modified DSM used for small width-to-thickness ratios (b/t = 35 and 40), on the contrary, it is underestimation when modified DSM applied to large width-to-thickness ratios (b/t = 60 and 70).

4.2.2 EYSM

EYSM was first proposed by Little (1979). Subsequently, in more than twenty years, it developed very slowly. Until 2009, it has been further improved by Chen. In his study, Chen (2009) argued that there was an identity between EYSM and EWM, and EWM would be replaced by EYSM because of its simplification of calculation. As a result, EWM is not included herein and only EYSM is repeated again.

The effective yield strength, f_{ye}, by EYSM, is given as follows

$$f_{ye} = \rho f_y \tag{9}$$

where ρ is the effective yield strength coefficient, and is calculated using the following formulas.

$$\rho = 1 \qquad \text{for} \qquad \lambda_p \le 0.746 \tag{10a}$$

$$\rho = \frac{1}{\lambda_p}\left(1 - \frac{0.19}{\lambda_p}\right) \qquad \text{for} \qquad \lambda_p > 0.746 \tag{10b}$$

in which, λ_p is the equivalent plate slenderness ratio, and given by Eq. (11) or (12)

$$\lambda_p = \sqrt{f_y / \sigma_{cr,p}} \tag{11}$$

$$\lambda_p = \sqrt{\varphi f_y / \sigma_{cr,p}} \tag{12}$$

For a square box section, the critical stress of a plate, $\sigma_{cr,p} = \frac{4\pi^2 E}{12(1-v^2)}\left(\frac{t}{b}\right)^2$. Substitute it into Eqs. (11) and (12) and obtain

$$\lambda_p = \frac{b/t}{56.3}\sqrt{\frac{f_y}{23.5}} \tag{13}$$

or

$$\lambda_p = \frac{b/t}{56.3}\sqrt{\frac{\varphi f_y}{235}} \tag{14}$$

The load carrying capacity of a thin-walled compression member, N, will be calculated using the following equation.

$$N = \varphi A f_{ye} \tag{15}$$

where the factor, φ, obtained from the Code GB50017-2003 according to $\lambda\sqrt{f_{ye}/235}$ when Eq. (13) is used. In order to simplify the calculation, $\lambda\sqrt{f_{ye}/235}$ is replaced by $\lambda\sqrt{f_y/235}$ when Eq. (14) adopted. In all calculations, as mentioned above in Section 4.1.2, curve *a* is employed to get the value of φ.

The calculation results, N_1, according to Eq. (13), and N_2, to Eq. (14) are also listed in Tables 4-7, in which, the errors, $\varepsilon_3 = \frac{P_u - N_1}{N_1} \times 100\%$, and $\varepsilon_4 = \frac{P_u - N_2}{N_2} \times 100\%$. Large differences between the numerical and predicted results show that EYSM, especially in the case of using Eq. (13), underestimates the carrying capacities of welded box section columns with slender plates over a wide range of width-to-thickness ratios and steel grades.

5. Proposed modified DSM

5.1 Deficiency of DSM

DSM is more accurate in estimating the bearing capacities of welded square box compression members with large width-thickness ratios, compared to modified DSM and EYSM, over a wide range of width-thickness ratios, slenderness and steel grades. However, for SM58 steel as shown in Table 7, DSM overestimates the load-carrying capacities of the columns with b/t = 35 and 40. In order to confirm the conclusion, fifteen experimental results (Usami and Fukumoto 1982, 1984) about welded square section columns, failed in the local and overall interaction buckling, are selected, in Table 8, to check against the predicted results using DSM. The serial number of specimens is same as that in Table 1. Except for specimen S-10-58, the width-thickness ratios of the others, which range from 22 to 44, are not too large. Moreover, all the specimens are made of two kinds of high strength steels, some of HT80 steel, with nominal yield strength of 690 MPa and measured yield strength of 741 MPa, and some of SM58 steel. In Table 8, P_T is test result, P_{l3} represents the predicted value by DSM, and ε_5 is a relative error, $\varepsilon_5 = \frac{P_T - P_{l3}}{P_{l3}} \times 100\%$. It can be noticed that almost all of the differences, ε_5, are negative, indicating that the predicted results obtained from DSM are greater than the experimental results mostly. In a word, it is proved, whether from experimental or numerical results, that DSM isn't safe for high strength steel columns with nominal yield strength greater than 460 MPa and small width-thickness ratios. Hence, DSM is still need to be modified.

5.2 Modified DSM proposed in this paper

The curves of stability reduction factor, φ, against modified slenderness ratio, $\lambda\sqrt{f_y/235}$, for SM58 steel, obtained from numerical results, are plotted as shown in Fig. 5, in which, the range of slenderness ratio, λ, is enlarged up to 120, i.e., λ = 20, 40, 60, 80, 100 and 120. It can be found from Fig. 5 that the influences of width-thickness ratios, b/t, on the ultimate strengths are large when $\lambda < 80$ (corresponding to $\lambda\sqrt{f_y/235} \le 124$ in Fig. 5) and $b/t < 45$. On the other hand, the values of width-thickness ratios, as just discussed in Table 8, in the test (Usami and Fukumoto

Table 8 Comparison of experimental (Usami and Fukumoto 1982, 1984) and predicted results by DSM and proposed modified DSM

Specimen	P_T/ kN	P_{l3}/ kN	P_{l4}/ kN	ε_5/%	ε_6/%	Specimen	P_T/ kN	P_{l3}/ kN	P_{l4}/ kN	ε_5/%	ε_6/%
S-10-22	2445	2635.32	2515.29	-7.22	-2.79	S-35-44	2631	3014.07	2595.10	-12.71	1.38
S-10-27	2592	2809.42	2647.86	-7.74	-2.11	S-50-22	1798	1735.36	1735.36	3.61	3.61
S-10-33	2749	3005.35	2734.60	-8.53	0.53	S-50-27	2024	2214.23	2187.40	-8.59	-7.47
S-10-38	2744	3142.69	2768.16	-12.69	-0.87	S-50-33	2440	2428.64	2275.34	0.47	7.24
S-10-44	2813	3305.71	2797.45	-14.90	0.56	S-10-29	1280	1354.78	1285.02	-5.52	-0.39
S-35-22	2112	2175.47	2175.47	-2.92	-2.92	S-10-44	1190	1509.95	1318.34	-21.19	-9.74
S-35-33	2641	2791.67	2579.06	-5.40	2.40	S-10-58	1310	1666.41	1346.41	-21.39	-2.70
S-35-38	2602	2896.50	2590.29	-10.17	0.45						

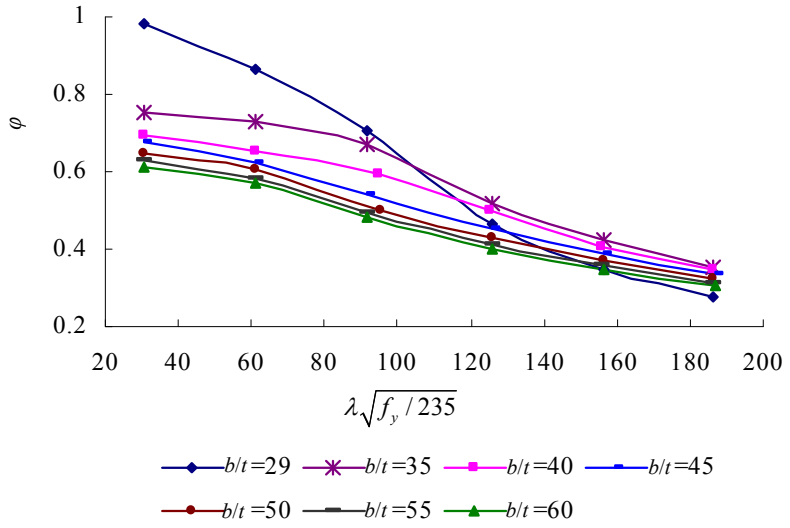

Fig. 5 Curves of columns for SM58 steel

1982, 1984) should also be considered. Therefore, the limiting value of width-thickness ratio, by which to determine whether DSM should be modified, may be adjusted from 40 to 45.

By trial and error, modifications of DSM are made as the following steps: (1) use the form of Eq. (3b) mentioned above for reference; (2) replace the coefficient of 0.15 with 0.22; (3) substitute the power exponent of 0.6 for 0.4; and (4) change the demarcation point, λ_l, from 0.776 to 0.658. Thus, for a welded thin-walled square shaped column with $b/t < 45$ and $\lambda < 80$, and made of high strength steel, the maximum strength should be checked as follows

$$\text{when} \quad \lambda_l \le 0.658 \qquad P_l = P_m \tag{16a}$$

$$\text{when} \quad \lambda_l > 0.658 \qquad P_l = \left[1 - 0.22\left(\frac{P_{cr,l}}{P_m}\right)^{0.6}\right]\left(\frac{P_{cr,l}}{P_m}\right)^{0.6} P_m \tag{16b}$$

Table 9 Comparison of calculated results by FEM and proposed modified DSM

b/t		35			40	
λ	P_{l5}/ kN	P_u/ kN	ε_7/%	P_{l5}/ kN	P_u/ kN	ε_7/%
20	1023.56	987.03	-3.57	1037.87	1038.27	0.04
40	970.56	953.80	-1.73	987.26	973.27	-1.42
60	845.98	877.78	3.76	868.47	884.37	1.83
80	631.85	674.03	6.68	684.11	745.58	8.99

The estimated results, P_{l4}, and corresponding errors, $\varepsilon_6 = \dfrac{P_T - P_{l4}}{P_{l4}} \times 100\%$, using modified DSM proposed in this study are also given in Table 8. The values of the differences, ε_6, range form -9.74% to 7.24%, and the proposed modified DSM is in excellent agreement with the experiment results. In addition, for b/t = 35 and 40 columns, having large errors when calculated by DSM and modified DSM as shown in Table 7, the calculation results, P_{l5}, obtained from proposed modified DSM are shown in the Table 9 and compared with the numerical results, P_u. The errors, $\varepsilon_7 = \dfrac{P_u - P_{l5}}{P_{l5}} \times 100\%$, are also listed in the Table 9. Similarly, the proposed modified DSM is in good agreement with the FEM simulated results.

In fact, the proposed modified DSM is consistence with EWM, especially for a welded square section. In order to compare with EWM, Eqs. (16a) and (16b) can be rewritten in the following form

$$\text{when} \quad \lambda_l \le 0.658 \qquad \frac{P_l}{A} = \varphi f_y \tag{17a}$$

$$\text{when} \quad \lambda_l > 0.658 \qquad \frac{P_l}{A} = \frac{1}{\lambda_{pl}}\left(1 - \frac{0.22}{\lambda_{pl}}\right)\varphi f_y \tag{17b}$$

where $\lambda_{pl} = (\varphi f_y / \sigma_{cr,l})^{0.6}$.

The effective width, b_e, which is based on Winter formula and adopted in NAS AISI 2001 and EN1993-1-5, is given as

$$\text{when} \quad \lambda_p \le 0.673 \qquad b_e = b \tag{18a}$$

$$\text{when} \quad \lambda_p > 0.673 \qquad b_e = \frac{1}{\lambda_p}\left(1 - \frac{0.22}{\lambda_p}\right)b \tag{18b}$$

where $\lambda_p = (f_{\max} / \sigma_{cr,p})^{0.5}$, in which $f_{\max}$ is the maximum stress of a plate.

Obviously Eqs. (17a) and (17b) are expressed in the same way as Eqs. (18a) and (18b) except that the exponent of 0.5 is replaced by a value of 0.6. The exponent of 0.6 is same as that given in the Modified Winter approach proposed by Pircher *et al*. (2002) when a welded square steel tube section with f_y = 282 MPa was investigated, but the coefficient of 0.22 is different from the value of 0.25 proposed by Pircher *et al*. (2002). The increase of the exponent from 0.5 to 0.6 is reason-

able, since the adverse effect of initial imperfections is smaller on the columns with welded square sections than those with cold-formed ones due to the favorable distribution of residual stress and the smaller amplitude of initial curvature.

6. Conclusions

A double nonlinear finite element model taking account of both the geometric and material imperfections was developed by using the ANSYS program. The ultimate bearing capacities of medium and high strength steel welded square section columns with slender plates are analyzed by the proposed finite element model. Comparisons between the numerical and the predicted results using DSM, modified DSM and EYSM, are also performed. The following conclusions can be drawn from this study:

- The finite element model proposed in this paper can simulate the nonlinear local-overall interaction buckling behavior of welded box section columns under axial compression very well.
- A suggestion is made that, in the case of $b/t > 20$, curve *a*, rather than curve *b* provided in GB50017-2003 should be used to check the global stability of welded square section columns fabricated from Q345, Q390, Q420, and SM58 steels. And thus, curve *a* is used for checking the local-overall interaction buckling strength of welded square section columns fabricated from medium and high strength steels when using DSM, modified DSM and EYSM.
- There are large differences between the numerical and the calculation results according to EYSM, and this approach is conservative.
- DSM provides a better prediction of the ultimate carrying capacities of welded square box compression members with large width-thickness ratios, compared to modified DSM and EYSM, over a wide range of width-thickness ratios, slenderness and steel grades. However, for high strength steels (nominal yield strength is greater than 460 MPa), the existing experimental and numerical results indicate that DSM overestimates the load-carrying capacities of the columns with $b/t < 45$ and $\lambda < 80$.
- The proposed modified DSM, for high strength steel columns with $b/t < 45$ and $\lambda < 80$, is in excellent agreement with the experimental and numerical results. In the meantime, the proposed modified DSM is consistence with the EWM.

Acknowledgments

The research reported in the paper is the project supported by the Research Foundation of Education Bureau of Shaanxi Province, China (Grant No. 2013JK0978), and the project supported by National Science Basic Research Plan in Shaanxi Province, China (Grant No. 2013JM7008). Their financial support is highly appreciated.

References

American Iron and Steel Institute (AISI) (2001), North American Specifications for the Design of Cold-Formed Steel Structural Members, Washington D.C., USA.

American Iron and Steel Institute (AISI) (2004), Supplement 2004 to the North American Specifications for the Design of Cold-Formed Steel Structural Members, Washington D.C., USA.
Becque, J. and Rasmussen, Kim J.R. (2009), "A numerical investigation of local-overall interaction buckling of stainless steel lipped channel columns", *J. Constr. Steel Res.*, **65**(8-9), 1685-1693.
Becque, J., Lecce, M. and Rasmussen, Kim J.R. (2008), "The direct strength method for stainless steel compression members", *J. Constr. Steel Res.*, **64**(11), 1231-1238.
Chen, S.F. (1992), *Steel Structures*, China Architecture & Building Press, Beijing, China. [In Chinese]
Chen, S.F. (2009), "Capacity calculation of welded axially compressed members with thin-walled box section", *Prog. Steel Build. Struct.*, **11**(6), 1-7. [In Chinese]
de Miranda Batista, E. (2009), "Local-global buckling interaction procedures for the design of cold-formed columns: Effective width and direct method integrated approach", *Thin-Wall. Struct.*, **47**(11), 1218-1231.
Degée, H., Detzel, A. and Kuhlmann, U. (2008), "Interaction of global and local buckling in welded RHS compression members", *J. Constr. Steel Res.*, **64**(8-9), 755-765.
EN 1993-1-1 (2005), Design of Steel Structures-Part 1-1: General rules and rules for buildings.
GB 50017-2003 (2003), Code for Design of Steel Structures, Beijing.
Georgieva, I., Schueremans, L., Vandewalle, L. and Pyl, L. (2012), "Design of built-up cold-formed steel columns according to the direct strength method", *Procedia Eng.*, **40**, 119-124.
Guo, Y.L. (1992), "Ultimate load behavior of welded thin-walled stub columns under combined loading of axial compression and bending", *Comput. Struct.*, **42**(4), 591-597.
Kwon, Y.B., Kim, N.G. and Hancock, G.J. (2007), "Compression tests of welded section columns undergoing buckling interaction", *J. Constr. Steel Res.*, **63**(12), 1590-1602.
Landesmann, A. and Camotim, D. (2013), "On the Direct Strength Method (DSM) design of cold-formed steel columns against distortional failure", *Thin-Wall. Struct.*, **67**, 168-187.
Little, G.H. (1979), "The strength of square steel box columns-design curves and their theoretical basis", *Struct. Engr.*, **57A**(2), 49-61.
Pircher, M., O'Shea, M.D. and Bridge, R.Q. (2002), "The influence of the fabrication process on the buckling of thin-walled steel box sections", *Thin-Wall. Struct.*, **40**(2), 109-123.
Rusch, A. and Lindner, J. (2001), "Remarks to the direct strength method", *Thin-Wall. Struct.*, **39**(9), 807-820.
Schafer, B.W. (2008), "Review: The direct strength method of cold-formed steel member design", *J. Constr. Steel Res.*, **64**(7-8), 766-778.
Shen, H.X. (2012), "Ultimate capacity of welded box section columns with slender plate elements", *Steel Compos. Struct., Int. J.*, **13**(1), 15-33.
Shahbazian, A. and Wang, Y.C. (2011), "Application of the direct strength method to local buckling resistance of thin-walled steel members with non-uniform elevated temperatures under axial compression", *Thin-Wall. Struct.*, **49**(12), 1573-1583.
Shahbazian, A. and Wang, Y.C. (2012), "Direct strength method for calculating distortional buckling capacity of cold-formed thin-walled steel columns with uniform and non-uniform elevated temperatures", *Thin-Wall. Struct.*, **53**, 188-199.
Sputo, T. and Tovar, J. (2005), "Application of direct strength method to axially loaded perforated cold-formed steel studs: Longwave buckling", *Thin-Wall. Struct.*, **43**(12), 1852-1881.
Swanson Analysis Systems Inc. (2004), *Ansys Reference Manual*, version 8.1.
Tovar, J. and Sputo, T. (2005), "Application of direct strength method to axially loaded perforated cold-formed steel studs: Distortional and local buckling", *Thin-Wall. Struct.*, **43**(12), 1882-1912.
Usami, T. and Fukumoto, Y. (1982), "Local and overall buckling of welded box columns", *J. Struct. Div.*, **108**(ST3), 525-542.
Usami, T. and Fukumoto, Y. (1984), "Welded box compression members", *J. Struct. Eng.*, **110**(10), 2457-2470.

CC

Nomenclature

A	cross-section area
b	plate width
b_e	plate effective width
c	distribution length of tensile residual stresses
E	Young's modulus
f_y	steel yield strength
f_{ye}	effective yield strength
$f_{\max}$	maximum stress of a plate
h	cross-section depth
h_0	distance between the centre lines of the two opposite plates
l	column length
m	buckling half-wave number along the axial direction (z-direction)
N, N_1, N_2	load-carrying capacity according to EYSM
P_u	numerical result
$P_{cr,l}$	critical local buckling load
P_l	column strength
P_{l1}, P_{l3}	load-carrying capacity calculated using DSM
P_{l2}	load-carrying capacity calculated using modified DSM
P_{l4}, P_{l5}	load-carrying capacity calculated using proposed modified DSM
P_m	overall stability capacity of a column
P_T	experimental result
i	governing radius of gyration
t	plate thickness
t_w	web thickness
U_z	translation in z direction
x, y, z	coordinate axis
λ	member slenderness ratio
λ_p	non-dimensional plate slenderness ratio
λ_{pl}	a parameter, and $\lambda_{pl} = (\varphi f_y / \sigma_{cr,l})^{0.6}$
λ_l	a parameter, and $\lambda_l = \sqrt{P_m / P_{cr,l}}$
φ, φ_1, φ_2, φ_3, φ_4, φ_5	overall stability coefficient of an axially compressed member

φ_a, φ_b	overall stability factor corresponding to curve *a* and *b* recommended in Code GB50017-2003
ρ	effective yield strength coefficient
σ_{rc}	compressive residual stress
$\sigma_{cr,l}$, $\sigma_{cr,p}$	critical buckling stress of a plate
ω	plate local initial deflection
ω_0	amplitude of local buckling, and $\omega_0 = b/1000$
v	Poisson's ratio
ε_1, ε_2, ε_3, ε_4, ε_5, ε_6, ε_7	relative error